The American Journal of Human Genetics, Volume *107*

Supplemental Data

Enhanced MAPK1 Function Causes a Neurodevelopmental Disorder within the RASopathy Clinical Spectrum

Marialetizia Motta, Luca Pannone, Francesca Pantaleoni, Gianfranco Bocchinfuso, Francesca Clementina Radio, Serena Cecchetti, Andrea Ciolfi, Martina Di Rocco, Mariet W. Elting, Eva H. Brilstra, Stefania Boni, Laura Mazzanti, Federica Tamburrino, Larry Walsh, Katelyn Payne, Alberto Fernández-Jaén, Mythily Ganapathi, Wendy K. Chung, Dorothy K. Grange, Ashita Dave-Wala, Shalini C. Reshmi, Dennis W. Bartholomew, Danielle Mouhlas, Giovanna Carpentieri, Alessandro Bruselles, Simone Pizzi, Emanuele Bellacchio, Francesca Piceci-Sparascio, Christina Lißewski, Julia Brinkmann, Ronald R. Waclaw, Quinten Waisfisz, Koen van Gassen, Ingrid M. Wentzensen, Michelle M. Morrow, Sara Álvarez, Mónica Martínez-García, Alessandro De Luca, Luigi Memo, Giuseppe Zampino, Cesare Rossi, Marco Seri, Bruce D. Gelb, Martin Zenker, Bruno Dallapiccola, Lorenzo Stella, Carlos E. Prada, Simone Martinelli, Elisabetta Flex, and Marco Tartaglia

SUPPLEMENTAL DATA

Case Reports

Figure S1. Multiple protein sequence alignment among MAPK1 orthologs and MAPK3.

Figure S2. Tolerance landscape of genetic variation for *MAPK1*.

Figure S3. The evolving phenotype of Subject 2 with age.

Figure S4. MAPK and RSK phosphorylation assays performed in primary fibroblasts from Subject 2 (p.Asp318Gly).

Figure S5. RASopathy-causing MAPK1 proteins show a variably enhanced nuclear translocation in response to EGF stimulation.

Figure S6. Endogenous MAPK1^{D318G} less efficiently co-immunoprecipitates with MKP3 and retains dependence on MEK activity in upregulating MAPK signaling.

Table S1. WES info and statistics.

Table S2. WES data output.

Table S3. Clinical features of subjects with *de novo* pathogenic *MAPK1* variants.

Table S4. Vulval phenotypes in *mpk-1*(*pan14*[D321G]) knock-in *C. elegans* hermaphrodites and in worms overexpressing a subset of disease-causing *MAPK1* mutant alleles under the control of p*lin-31*.

Case Reports

Subject 1 (p.Ala174Val), a male, is the only child of healthy, non-consanguineous Italian parents. The age of parents at birth was 30 years. Family history was unremarkable. He has one healthy half-sister (21 years old) and one half-brother (4 years old). He was born at 41 weeks of gestation by Cesarean section after an uneventful pregnancy. Birth weight was 3,650 g (+0.6 SD) and length 53 cm (+1.65 SD). OFC and Apgar scores were not available. Perinatal period was normal. Developmental milestones were mildly delayed (he walked alone at 18 months, first words reported at 12 months). He presented fine motor delay and atypical social behaviors characterized by anxiety and reduced stress tolerance. At 6 years, mitral regurgitation with mitral valve prolapse and patent foramen ovale was noted. Clinical evaluation at 13 years disclosed curly and thick hair, epicanthal folds, mild hypertelorism, blue eyes, low-set posteriorly rotated ears, multiple lentigines, pterygium colli, scapular winging, cubitus valgus, and bilateral pes planus. He has myopia corrected with lens. At the last evaluation, the height was 157 cm (-0.04 SD), weight 45.5 kg (-0.01 SD) and OFC 59 cm (+2.82 SD). Extensive genetic analyses, including array-CGH and a large panel of RASopathy genes, were normal.

Subject 2 (p.Asp318Gly) was born at 40 weeks of gestation following an uneventful pregnancy and delivery. Birth weight was 3,350 g (-0.6 SD), length 47 cm (-2.28 SD), head circumference 33 cm (-1.75 SD). The parents were not consanguineous, and the family history was unremarkable. Neonatal transition was normal. At 2 years, he was referred to our unit for growth retardation and mild psychomotor delay. Physical examination revealed brachicephaly, hypertelorism, epicanthal folds, downslanting palpebral fissures, bilateral ptosis, low-set posteriorly rotated ears, wide nasal bridge, prominent and pointed chin, a low posterior hairline, mild hypotonia, one cafè-au-lait spot, and three hypochromic spots. Peripheral lymphedema was also observed. Echocardiography showed an atrial septal defect, which later resolved spontaneously and mild mitral valve prolapse, which was not hemodynamically relevant. Abdominal and renal sonography were normal. He had mild psychomotor delay, moderate intellectual disability with a learning disorder and graphomotor and praxic constructive skills deficit. He received rehabilitative physical therapy and speech therapy. Pharmacological therapy was also administered to treat his ADHD. Cerebral MRI showed cavum septum pellucidum. Results of ophthalmologic and ENT evaluations were normal. He presented with bilateral pes planus and mild legs asymmetry (5 mm). He underwent surgery for monolateral cryptorchidism and hypospadia. At age 3 years, partial GH deficiency was diagnosed, and he was treated with GH therapy. At the auxological follow-up (12 years), height had increased to 25th centile and the pubertal growth spurt had started.

Subject 3 (p.His80Tyr), a male, was born at 39 weeks of gestation. The pregnancy had been complicated by slightly increased nuchal translucency (3.8 mm at 12 weeks). Amniocentesis showed a normal karyotype. Birth weight was 3,672 g (+0.5 SD), length 50 cm (0 SD), head circumference 34.5 cm (0 SD), APGAR score 8/10/10 at 1, 5 and 10 minutes, respectively. The neonatal period had been complicated by transient tachypnea and feeding problems that required tube feeding for one month. At 1 month of age, brain MRI showed mild widening of frontal peripheral fluid spaces. A suspicion of seizures was ruled out by a normal EEG pattern. Developmental milestones were delayed (rolled over at 9 months, sit almost independently at 12 months, crawling at 18 months, walking at 30 months). Sleeping problems had already been recorded at 6 months. Speech was delayed

at 2 years of age. He had chronic middle ear effusions and received ear tubes. Audiologic investigations were difficult, because of behavioral problems but did not show hearing loss. Clinical evaluation at 6 years of age revealed frustrated and aggressive behavior, head-banging, spitting and hitting, language delay (few words, no sentences) and an easy bruising. He was diagnosed with celiac disease. Growth parameters were impaired (height: 105 cm, -3 SD; weight: 17.4 kg, -2 SD; OFC: 48.5 cm; -2 SD). The dysmorphological evaluation evidenced a high forehead, medially thin and flaring eyebrows, posteriorly rotated ears, round nasal tip, upturned nostrils, small teeth with fusion of two teeth, broad thorax, flat feet and bruises at arms and legs. The follow-up evaluation at 9 years of age confirmed the intellectual disability and language delay (few words). Behavior problems were confirmed, although slightly improved. He had a dry skin (especially at the back of upper arms). No heart malformation was detected by echocardiography at 6 years of age. Genetic and metabolic testing including Prader-Willi syndrome methylation profile, chromosomal microarray, UPD14 and fragile X-syndrome were normal.

Subject 4 (p.Asp318Asn) is a 17 year-old female, first child of healthy non-consanguineous Dutch parents. Premature rupture of the membranes occurred at 30 weeks gestation, but pregnancy was otherwise normal. A Caesarean section was performed (37 weeks of gestation) because of breech position. Birth weight was 2,610 g (10th-50th centile). Length, OFC and Apgar scores were not available. Perinatal period was uncomplicated. Developmental milestones were delayed. She walked independently when she was 20 months old. At 3 years, she spoke single words only. Ear tubes were inserted and speech therapy was initiated. By age 4, she used 3 to 4 words per sentence, but her speech was difficult to understand. At the age of 9 years, her total IQ score was 64, with a verbal IQ of 71 and a nonverbal IQ of 61. She could read and write some words, and could get dressed and eat independently. She attends a school for special education. She was diagnosed with ADHD, which has been treated with methylphenidate. At the age of 16 years, Tietze syndrome was diagnosed. Clinical evaluation disclosed a broad forehead, dark broad horizontal eyebrows, hypertelorism, short and almond-shaped palpebral fissures, thick vermillion of the upper and lower lip, slightly posterior rotated ears, low posterior hairline, hypertrichosis, a broad thorax and a hoarse voice. At the last evaluation, her height was 163 cm (-0.87 SD) and weight was 53.5 kg (-0.5 SD). Echocardiography showed mitral valve billowing. Biochemical and metabolic screening were normal, as was testing of *FMR1* and *ABCC9.* Array-CGH revealed a paternally inherited duplication of 2q12.3q13 (~310 Kb).

Subject 5 (p.Pro323Arg) was a male born at 41 weeks gestational age *via* SVD after uncomplicated pregnancy. Mother was a 37 year-old G5P4 and father was 40 years old. He had a normal newborn metabolic screen. He was diagnosed with an atrial septal defect by echocardiogram. At 4 months of age, he presented with seizures and was admitted to the hospital. EEG was consistent with infantile spasms. He was treated with vigabatrin with good response. At age 1 year, he has been seizure free with a normal repeated EEG. At 4 months, brain MRI did not identify congenital malformations. The patient had multiple admissions for pneumonia, later on diagnosed with aspiration culture. A gastrostomy tube was placed at 14 months. He is primarily fed via this tube but can eat solids and thickened liquids by mouth. He was also diagnosed with a right duplicated kidney collecting system by ultrasound. Developmental delay was suspected at age 8 months. He rolled over at age 8 months, sat unassisted at age 10 months, crawled at 19 months, and walked at 27 months. He has few words and was diagnosed with speech apraxia. He also has difficulty

in communication and interaction and has an aggressive behavior. He cannot sit still for any period, and is not interested in socializing. Behavior is in the autism spectrum disorder, which is treated with ABA therapy. No sleep difficulties have been reported. He is not toilet trained yet. Genetic testing, including SNP chromosomal microarray, lysosomal studies, and urine studies for organic acids and mucopolysaccharides provided normal results.

Subject 6 (p.Glu322Gln), a male, is the third child of healthy parents. At birth he came to medical attention because of multiple dysmorphic features including bilateral clubfeet, hypotonia, ptosis and cryptorchidism, though no genetic testing was performed. He was the 3,060 g product of a 38 weeks gestation born *via* SVD to a 26-year-old G3P3 female whose pregnancy was said to be uncomplicated. He was evaluated at 2 years for his very poor growth and global delays and again at age 5, when he underwent testing to include a chromosomal microarray, serum 7-DHC, PWS methylation testing, metabolic studies and a Noonan syndrome gene panel, all of which were normal. The parents were told that the child likely had a form of Noonan syndrome. He has been lost to genetics follow-up until 2019 when he underwent a new evaluation, primarily due to parental concern about Crohn's disease affecting growth at age 15. Examination at that time revealed severe growth retardation with all parameters measuring well below the 1st percentile. Dysmorphic features included trigonocephalic skull, large pinnae with superior protrusion and posterior rotation, severe bilateral ptosis with downslanting palpebral fissures, long fine eyelashes with arched brows, malar hypoplasia, myopathic mouth and retrognathia. The child appeared hirsute and was severely delayed, non-verbal and non-ambulatory. Attempts to repair his ptosis have been unsuccessful.

Subject 7 (p.Ile74Asn) was an 8-year-old male, who was referred to clinic at the age of 3 because of psychomotor delay. He is the first child of non-consanguineous healthy parents of Spanish origin. He was born at 38 weeks via an uncomplicated vaginal delivery of a twin pregnancy (bicorial and biamniotic). Birth weight was 2,170 g (<3rd centile). There was no relevant family history. His brother is healthy. Global psychomotor retardation was clear from the first months of life. Clinical examination revealed low growth rate and dysmorphic features (*i.e.*, low hair implantation, downslanting palpebral fissures, hypertelorism, bulbous nose, prominent chin, short neck, short and puffy hands, tapered fingers, separated nipples, and wide thorax). At the age of 5 years, he started with valproic acid for the treatment of generalized seizures. Metabolic studies, karyotype, CGH-arrays and brain MRI were normal. EEG studies demonstrated the presence of generalized spikes and waves during sleep. We conducted a neuropsychological assessment to measure intellectual abilities. Tests revealed a full scale IQ of 53.

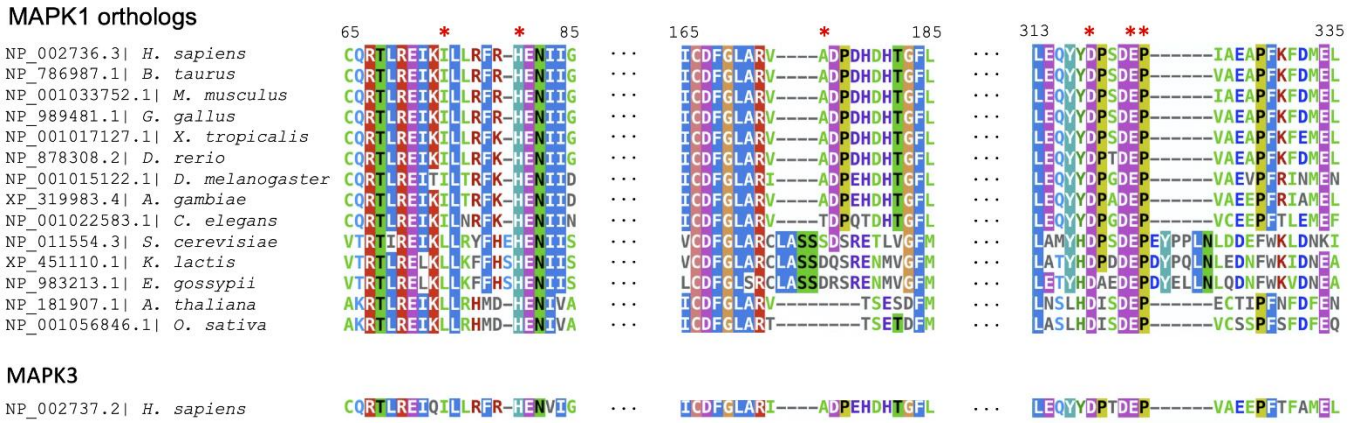

Figure S1. Multiple protein sequence alignment among MAPK1 orthologs and MAPK3.

Protein sequences from MAPK1 orthologs and human MAPK3 (also known as ERK1) were aligned by means of Muscle (v. 3.8) and visualized with MView (v.1.63). Background in consensus positions (identity >70%) is colored according to amino acid biochemical properties. Asterisks indicate the affected residues.

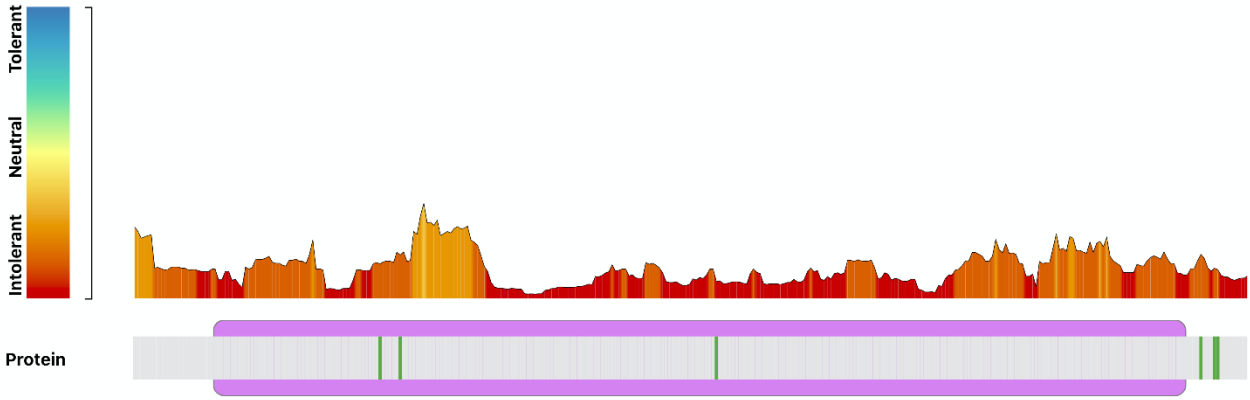

Figure S2. Tolerance landscape of genetic variation for *MAPK1*.

The histograms show the d_N/d_S ratio for individual residues, and are colored according to the scheme reported along the Y-axis. The protein sequence is depicted in grey with the kinase domain (PF00069) shown in violet. The residues affected by the disease-causing mutations identified in the study are shown in green.

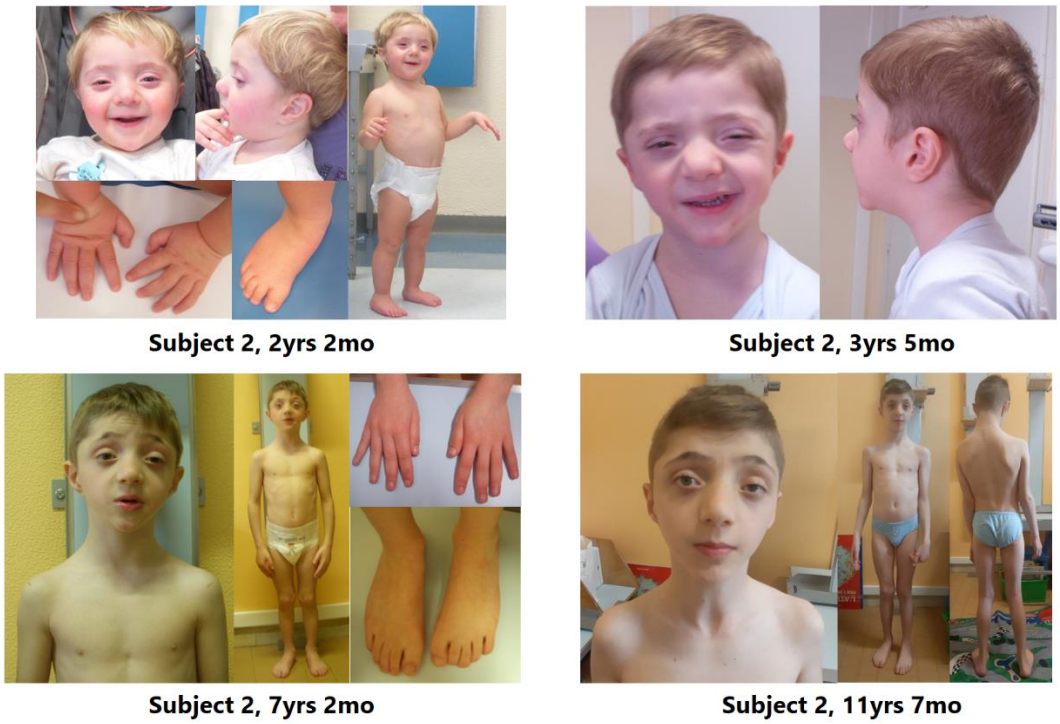

Figure S3. The evolving phenotype of Subject 2 with age.

Note: hypertelorism, downslanting palpebral fissures, bilateral ptosis, low-set posteriorly rotated ears, wide nasal bridge, prominent and pointed chin and distal lymphedema (2 years old); bitemporal narrowing, hypertelorism, downslanting palpebral fissures, bilateral ptosis, low-set posteriorly rotated ears, wide nasal bridge, prominent and pointed chin and low posterior hairline (3 years old); in addition to the facial features, note the pectus excavatum, cubitus valgus and bilateral pes planus (7 years old); bitemporal narrowing, hypertelorism, downslanting palpebral fissures, bilateral ptosis (left>right), low-set posteriorly rotated ears, wide nasal bridge, tubular nose, prominent and pointed chin, pectus excavatum, scapular winging, cubitus valgus and bilateral pes planus (11 years old).

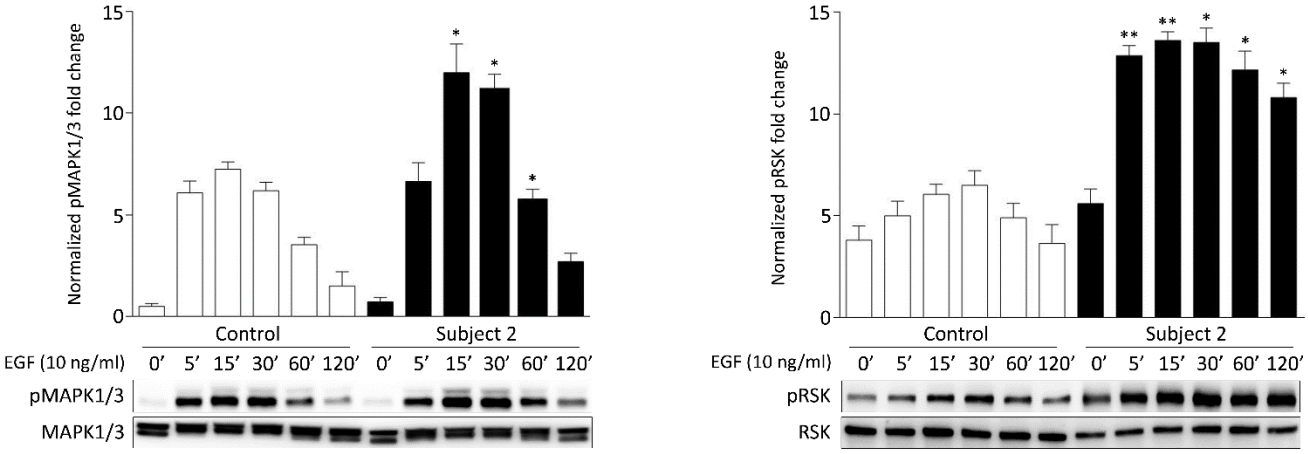

Figure S4. MAPK and RSK phosphorylation assays performed in primary fibroblasts from Subject 2 (p.Asp318Gly).

Representative blots (below) and graphs reporting mean ± SD densitometry values (above) of three independent experiments. Fibroblasts heterozygous for the *MAPK1* variant show higher MAPK1/3 (left) and RSK (right) phosphorylation levels compared to control cells. Cells were starved for 16 h and then stimulated with EGF (10 ng/ml), in time-course experiments, or left unstimulated. Equal amounts of cell lysates were resolved on 10% polyacrylamide gel. Asterisks indicate statistically significant differences in the phosphorylation levels compared to control cells at the corresponding experimental points (* $P<0.05$, ** $P<0.01$; Student's t-test).

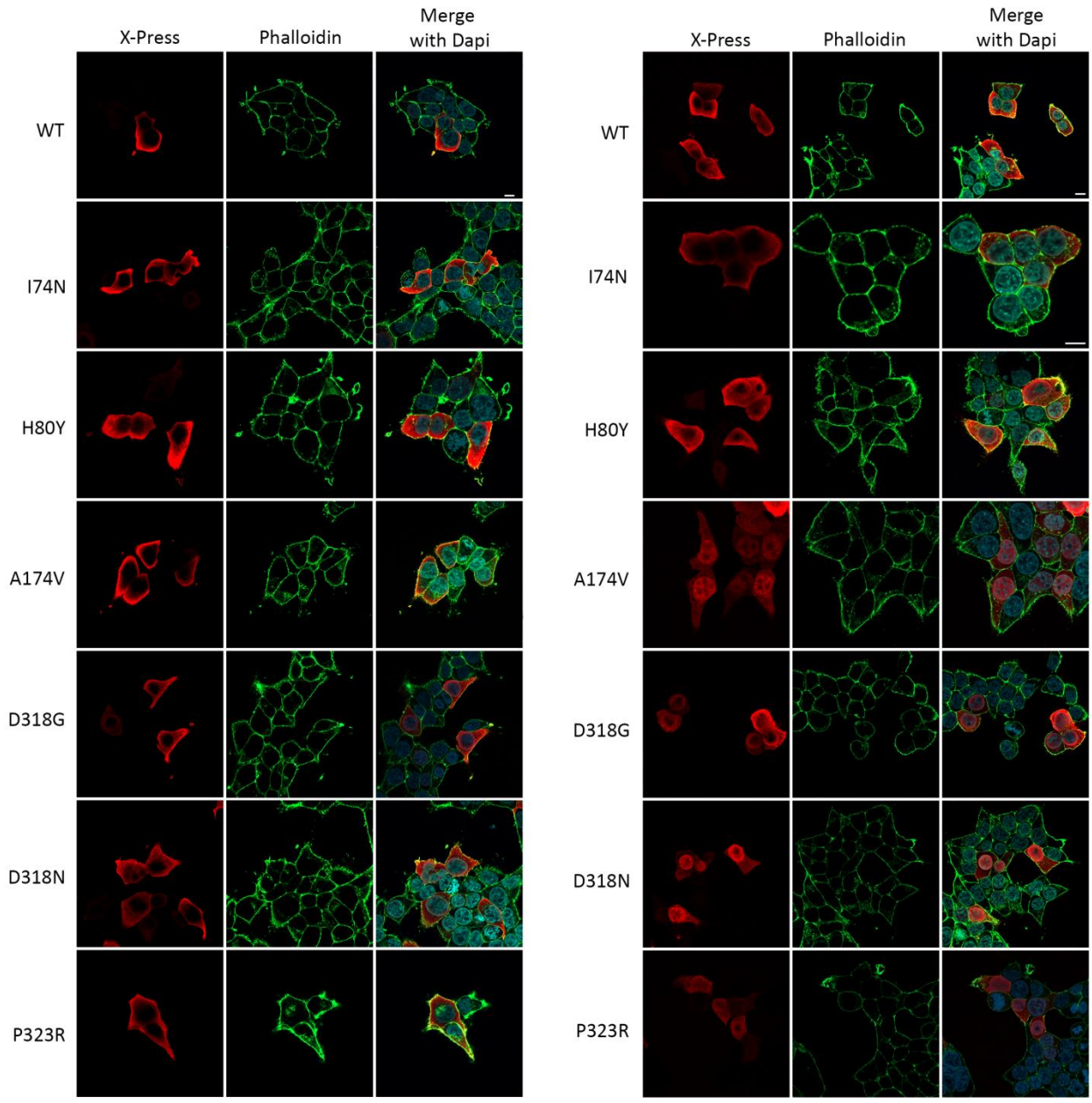

Figure S5. RASopathy-causing MAPK1 proteins show a variably enhanced nuclear translocation in response to EGF stimulation.

MAPK1 subcellular localization showed by confocal laser scanning microscopy observations. Panels represent central sections. Assays were performed in Lenti-X 293T cells transiently expressing Xpress-tagged wild-type and mutant *MAPK1* constructs. Fixed cells were stained with an anti-Xpress mouse monoclonal antibody followed by goat anti-mouse Alexa Fluor-594 (red), and an anti-phalloidin antibody conjugated to green-fluorescent Alexa Fluor 488 dye (green). Nuclei are visualized by DAPI staining (blue). Scale bar is 10 µm.

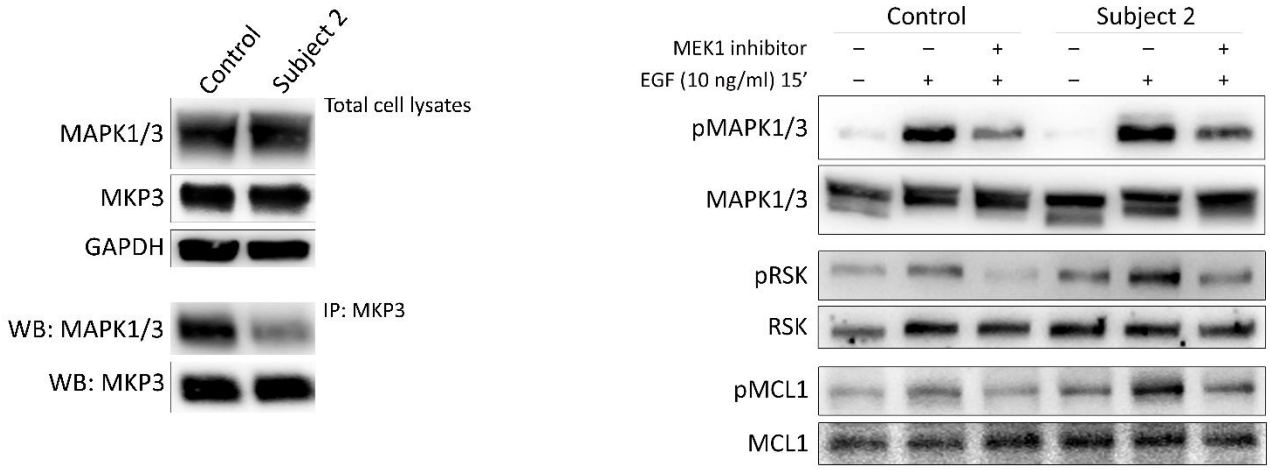

Figure S6. Endogenous MAPK1^{D318G} less efficiently co-immunoprecipitates with MKP3 and retains dependence on MEK activity in upregulating MAPK signaling.

The p.Asp318Gly substitution in MAPK1 impairs proper binding of MAPK1 to MKP3 (left panel). Lysates from primary fibroblasts (Subject 2) were immunoprecipitated with an anti-MKP3 antibody and assayed by western blotting using the indicated antibodies.

MAPK, RSK and MCL1 phosphorylation assays performed in primary fibroblasts (Subject 2) treated with the MEK inhibitor, trametinib (right panel). Assays were performed in cells starved for 16 h and stimulated with EGF (10 ng/ml, 15 min) after treatment with the MEK inhibitor, trametinib (1.5 ng/ml, 2 h). Blots show a comparable decrease in pMAPK, pRSK and pMCL1 in control and patient-derived cells in presence of trametinib, indicating that the mutation-driven signal upregulation of the MAPK cascade retains dependence on MEK activity.

Table S1. WES info and statistics.

ID	WES enrichment kit	Sequencing platform	Target regions covered >10x	Target regions covered >20x	Average depth on target
Subject 1	Agilent SureSelect Clinical Research Exome v2	NextSeq550	95%	91%	98x
Subject 2	Agilent SureSelect V6-All exons	HiSeq X Ten	>99%	98%	153x
Subject 3	Roche SeqCap EZ MedExome	HiSeq 2500	97%	94%	110x
Subject 4	Agilent SureSelect XT Exome v6	NextSeq500	97%	96%	145x
Subject 5	Agilent SureSelect Clinical Research Exome v1	HiSeq 4000	>99%	97%	91x
Subject 6	Agilent SureSelect XT Exome v6	HiSeq 4000	97%	96%	138x
Subject 7	Ion AmpliSeqTM Exome	Ion Proton	91%	83%	84x

Table S2. WES data output.

Subject 1	
Total number of high-quality variants	104,106
Number of variants with predicted functional effect[1]	15,875
Private, clinically associated, and unknown/low frequency variants[2]	268
Putative disease genes (recessive trait)[3]	1[4]
- Filtered candidate genes	none
Putative disease genes (dominant trait)[3]	4[5]
- Filtered candidate genes	*MAPK1*
Subject 2	
Total number of high-quality variants	113,892
Number of variants with predicted functional effect[1]	17,326
Novel, clinically associated, and unknown/low frequency variants[2]	287
Putative disease genes (recessive trait)[3]	none
- Filtered candidate genes[3]	none
Putative disease genes (dominant trait)[3]	4[6]
- Filtered candidate genes	*MAPK1*
Subject 3	
Total number of high-quality variants	86,724
Number of variants with predicted functional effect[1]	27,995
Novel, clinically associated, and unknown/low frequency variants[2]	970
Putative disease genes (recessive trait)[3]	2[7]
- Filtered candidate genes	none
Putative disease genes (dominant trait)[3]	2[8]
- Filtered candidate genes	*MAPK1*
Subject 4	
Total number of high-quality variants	83,499
Novel, clinically associated, and unknown/low frequency variants[2]	1,844
Number of variants with predicted functional effect[1]	707
Putative disease genes (recessive trait)[3]	none
- Filtered candidate genes	none
Putative disease genes (dominant trait)[3]	1[9]
- Filtered candidate genes	*MAPK1*
Subject 5	
Total number of high-quality variants	128,509
Number of variants with predicted functional effect[1]	18,852
Novel, clinically associated, and unknown/low frequency variants[2]	239
Putative disease genes (recessive trait)[3]	none
- Filtered candidate genes	none
Putative disease genes (dominant trait)[3]	2[10]
- Filtered candidate genes	*MAPK1*

Subject 6	
Total number of high-quality variants	357,113
Number of variants with predicted functional effect[1]	39,981
Novel, clinically associated, and unknown/low frequency variants[2]	79
Putative disease genes (recessive trait)[3]	none
- Filtered candidate genes	none
Putative disease genes (autosomal dominant trait)[3]	2[11]
- Filtered candidate genes	*MAPK1*
Subject 7	
Total number of high-quality variants	130.9732
Number of variants with predicted functional effect[1]	52.206
Novel, clinically associated, and unknown/low frequency variants[2]	327
Putative disease genes (recessive trait)[3]	6[12]
- Filtered candidate genes[3]	none
Putative disease genes (autosomal dominant trait)[3]	2[13]
- Filtered candidate genes	*MAPK1*

[1]High-quality non-synonymous SNVs/indels within coding exons and splice regions (-/+8) (subjects 1 and 2); high-quality SNVs/indels within coding exons and splice regions (-/+6) (subject 3); high-quality non-synonymous SNVs/indels within coding exons and splice regions (-/+20) (subject 4); high-quality non-synonymous SNVs/indels within coding exons and splice regions (-13/+6) (subject 5); high-quality non-synonymous SNVs/indels within coding exons and splice regions (-/+30) (subject 6); high-quality non-synonymous SNVs/indels within coding exons and splice regions (-/+5) (subject 7).

[2]High-quality non-synonymous SNV/indels within coding exons and splice regions with gnomAD MAF <0.1% and <1% in public (gnomAD) and in-house (~2,000 population-matched exomes) database (subjects 1 and 2); high-quality SNVs/indels within coding exons and splice regions (-/+6) with MAF <1% ESP6500, dbSNP and in house (~400 exomes, healthy subjects) databases (subject 3); high-quality non-synonymous SNVs/indels within coding exons and splice regions (-/+20) with MAF <1% in public (ExAC) and in-house (860 exomes, healthy subjects) databases (subject 4); high-quality non-synonymous SNVs/indels within coding exons and splice regions with MAF <1% (gnomAD) and <0.1% in-house (~200,000 exomes) databases (subject 5); high-quality non-synonymous SNVs/indels within coding exons and splice regions (-/+10) with MAF <1% in the ExAC database (subject 6); high-quality non-synonymous SNV/indels within coding exons and splice regions with MAF <1% in public (gnomAD) and in-house (~1,200 exomes) databases (subject 7).

[3]Functional impact assessed by Combined Annotation Dependent Depletion (CADD) v.1.4 (http://cadd.gs.washington.edu/), Mendelian Clinically Applicable Pathogenicity (M-CAP) v.1.0 (http://bejerano.stanford.edu/mcap/) and Intervar (http://wintervar.wglab.org) v2.0.1. Variants predicted as benign or likely benign by Intervar were discarded and only those with CADD score >15 or M-CAP score>0.025 were retained (subjects 1, 2 and 5); functional impact assessed using Alamut Visual (Interactive biosoftware) and literature (subject 3); variants were annotated, filtered and prioritized using the Bench NGS Lab platform (Agilent, Leuven, Belgium), functional impact was assessed using Alamut Visual (Interactive biosoftware) and literature (subject 4); functional impact assessed considering 8 predictor systems (SIFT, PROVEAN, MutationTaster, MutationAssessor, LRT, FATHMM, FATHMM-MKL, MetaSVM, MetaLR, GERP,) included in the Varsome engine (https://varsome.com). Private/rare/known

ClinVar pathogenic variants were classified following ACMG criteria (subject 6); functional annotation of the private/rare and HGMD/ClinVar pathogenic variants, was performed by combining 8 predictor systems (SIFT, PolyPhen2, MutationTaster, MutationAssessor, LRT, FATHMM, MetaSVM and CONDEL) included in the ALAMUT (http://www.interactive-biosoftware.com) and ANNOVAR (http://www.openbioinformatics.org/annovar/) packages. Variant categorization was performed following *ACMG* criteria (subject 7).

[4]*DNAH10* (c.1742G>A, p.Arg581Gln; c.13308A>T, p.Arg4436Ser), *TSPYL2* (c.611G>A, p.Ser204Asn, chr X).

[5]*CAPN14* (c.1279-2A>T, splice acceptor variant), *DOC2A* (c.151_152insC, p.Glu51fs), *MAPK1* (c.521C>T, p.Ala174Val), *WIPF2* (c.530_531insGG, p.Pro178fs).

[6]*ADH1B* (c.695G>A, p.Arg232Gln), *HYDIN* (c.11650G>A, p.Glu3884Lys), *KLK12* (c.328C>T, p.Arg110Trp), *MAPK1* (c.953A>G, p.Asp318Gly).

[7]*KLHL10* (c.454T>C, p.Tyr152His; c.887T>C p.Ile296Thr), *ZNF235* (c.424C>G, p.Gln142Glu; c.767T>G, p.Ile256Ser).

[8]*MAPK1* (c.238C>T, p.His80Tyr), *KIAA0368* (c.2407C>T, p.Arg803Trp).

[9]*MAPK1* (c.952G>A, p.Asp318Asn).

[10]*MAPK1* (c.968C>G, p.Pro323Arg), *CACNA1A* (c.6683 G>T, p.Arg2228Leu).

[11]*MAPK1* (c.964G>C, p.Glu322Gln), *MYH3* (c.720C>A, p.Asp240Glu).

[12]*AHNAK2* (c.12374_12376delATG insGCA p.Asp4125_Val4126delinsGlyMet; c.10274C>T, p.Ala3425Val)*, ARHGEF40* (c.1163G>A, p.Arg388Gln; c.2500C>T, p.Arg834Cys), *MAP3K15 (c.806G>A, p.Arg269Gln ;* chr X), *RILPL1* (c.752G>A, p.Arg251Gln, homozygous change), *USP53* (c.1849C>T, p.Pro617Ser; c.2611G>C, p.Gly871Arg), *ZNF81 (c.923T>C, p.Val308Ala,* chr X).

[13]*MAPK1* (c.221T>A, p.Ile74Asn), *WDR48* (c.796C>G, p.His266Asp).

Table S3. Clinical features of subjects with *de novo* pathogenic *MAPK1* variants.

Case ID	Subject 1	Subject 2	Subject 3	Subject 4	Subject 5	Subject 6	Subject 7
Ethnicity	Caucasian	Caucasian	Caucasian	Caucasian	Caucasian	Caucasian	Caucasian
Sex	Male	Male	Male	Female	Male	Male	Male
Age at last examination	13 y 2 mo	12 y	6 y	16 y	3 y 2 mo	15 y	8 y
***MAPK1* variant**							
Genomic position	Chr22(GRCh37): g.22153389G>A	Chr22(GRCh37): g.22127175T>C	Chr22(GRCh37): g.22162017G>A	Chr22(GRCh37): g.22127176C>T	Chr22(GRCh37): g.22123608C>G	Chr22(GRCh37): g.22127164C>G	Chr22(GRCh37): g.22162034 A>T
cDNA change (NM_002745.4)	c.521C>T	c.953A>G	c.238C>T	c.952G>A	c.968C>G	c.964G>C	c.221T>A
Amino acid change	p.Ala174Val	p.Asp318Gly	p.His80Tyr	p.Asp318Asn	p.Pro323Arg	p.Glu322Gln	p.Ile74Asn
Inheritance	*de novo*	*de novo*	*de novo*	*de novo*	*de novo*	*de novo*	*de novo*
gnomAD	not reported	not reported	not reported	not reported	not reported	not reported	not reported
Growth at birth							
Height (SD)	53 cm (+1.65 SD)	47 cm (-2.28 SD)	50 cm (0 SD)	NA	50.8 cm (+0.48 SD)	50.2 cm (+0.17 SD)	47 cm (-1.52 SD)
Weight (SD)	3,650 g (+0.6 SD)	3,350 g (-0.6 SD)	3,672 g (+0.5 SD)	2,610 g (-0.6 SD)	3,657 g (+0.62 SD)	3,062 g (-0.6 SD)	2,170 g (-2.75 SD)
OFC (SD)	NA	33 cm (-1.32 SD)	34.5 cm (+0.66 SD)	NA	NA	NA	33.5 cm (-1.11 SD)
Growth at last examination				16 y (OFC 9y 5mo)		14 y 10 mo	
Height (SD)	157 cm (-0.04 SD)	144.6 cm (-0.82 SD)	105 cm (-2.23 SD)	163 cm (-1.27 SD)	89 cm (-2.21 SD)	122 cm (-5.92 SD)	111 cm (-2.88 SD)
Weight (SD)	45.5 kg (-0.01 SD)	30 kg (-1.99 SD)	17.4 kg (-1.26 SD)	53.5 kg (-0.9 SD)	12.8 kg (-1.13 SD)	16.1 kg (-7.77 SD)	18 kg (-2.65 SD)
OFC (SD)	59 cm (+2.82 SD)	52 cm (-1.01 SD)	48.5 cm (-2.39 SD)	54 cm (+0.47 SD)	48.5 cm (-1.34 SD)	44 cm (-7.4 SD)	48 cm (-3.25 SD)
Development							
DD	yes	yes	yes	yes	yes	yes	yes
ID	no	yes	yes	yes	yes	yes	yes
Language delay	no	yes	yes	yes	yes (speech apraxia)	yes	yes
Behavioral problems	anxiety and reduced stress tolerance	ADHD	aggressive, destructive, spitting, head banging	ADHD	very active, destructive, affectionate, ASD	occasionally aggressive	severe ADHD
Learning disorder	yes	yes	yes	yes	yes	yes	yes

Case ID	Subject 1	Subject 2	Subject 3	Subject 4	Subject 5	Subject 6	Subject 7
Neurological							
Hypotonia	no	yes	yes	no	no	yes (axial hypotone with increased distal tone)	yes
Epilepsy	no	no	no	no	yes (4mo, infantile spasms, controlled with vigabatrin)	no	yes (5y, generalized seizures, controlled with valproic acid)
CHD	mitral regurgitation, mitral valve prolapse, patent foramen ovale	ASD and mild mitral valve prolapse	no	mitral valve billowing	ASD	no	no
Skeletal anomalies	pes planus, scapular winging, cubitus valgus	pes planus, mild legs asymmetry (5 mm)	broad thorax, pes planus	broad thorax	tapered fingers, with broad bast at MP joints tapering to the distal phalanges, scapular winging	dextroconvex thoracolumbar scoliosis, dislocation/subluxation of the left femoral head, clinodactyly, overlapping toes, prominent heels, bilateral clubfoot, limited elbow extension	hyperlaxity, short and puffy hands and feet, tapered fingers, mild metatarsus varus
Facies	epicanthal folds, blue eyes, hypertelorism, low-set posteriorly rotated ears, webbed/short neck	prominent metopic ridge, bitemporal narrowing, hypertelorism, downslanting palpebral fissures, ptosis, low-set posteriorly rotated ears, wide nasal bridge, prominent and pointed chin, low posterior hairline	high forehead, medial thin and flaring of eyebrows, ptosis, slightly wide nasal bridge when younger, round nasal tip (upturned), posteriorly rotated ears, small teeth, fusion of two teeth, webbed/short neck	broad forehead, full eyebrows, hypertelorism, ptosis, short and almond-shaped palpebral fissures, posteriorly rotated ears, full lips, hypertrichosis, hoarse voice, low posterior hairline	hypertelorism, ptosis, wide mouth, full lips, small lower incisors, widely spaced teeth, webbed/short neck	microcephaly, plagiocephaly, highly arched eyebrow, long eyelashes, downslanted palpebral fissures, severe ptosis (unsuccessfully treated), malar hypoplasia, low-set posteriorly rotated ears, carp-shaped mouth, long philtrum, crowded teeth, mandibular micrognathia, coarse facies, generalized hirsutism, low posterior hairline	prominent metopic ridge, bitemporal narrowing, mild hypertelorism, downslanted palpebral fissures, ptosis, low-set posteriorly rotated ears, wide nasal bridge, high arched palate, widely spaced teeth, pointed chin, low posterior hairline, webbed/short neck

Case ID	Subject 1	Subject 2	Subject 3	Subject 4	Subject 5	Subject 6	Subject 7
Other features							
Skin and annexes	curly and thick hair, multiple lentigines	1 *cafè au lait* spot, 3 hypochromic spots	dry skin, mild eczema	hypertrichosis	dry skin	freckling (forehead), several 5-10 mm hyperpigmented macules (feet, dorsal), thin nails, hypertrichosis	no
Cryptorchidism	no	yes	no	no	no	yes	no
GER	no	no	wet lung syndrome	no	history of aspiration	yes	no
Recurrent Infections	no	no	yes (ears)	yes (ears)	no	no	no
Lymphatic involvement	no	periphery lymphedema	no	no	no	no	no
Bleeding/easy bruising	no	no	yes	no	no	no	no
Auditory issues	no	no	no	no	no	no	no
Others features				Tietze syndrome			
Imaging and laboratory findings							
MRI/CT	not performed	cavum setto pellucido	mild widening frontal peripheral liquor spaces (1 mo)	not performed	normal (4 mo)	not available	normal
Abdominal U/S	not performed	normal	normal	not performed	duplicated collecting system of the right kidney	suspicious for bowel malrotation, inflammatory bowel disease (Crohn's disease), marked atrophy of the left kidney	no

ADHD, attention deficit hyperactivity disorder; ASD (behavioral problems), autistic spectrum disorder; ASD (CHD), atrial septal defects; CHD, congenital heart defects; DD, developmental delay; ID, intellectual disability; OFC, occipitofrontal circumference.

Table S4. Vulval phenotypes in *mpk-1*(*pan14*[D321G]) knock-in *C. elegans* hermaphrodites and in worms overexpressing a subset of disease-causing *MAPK1* mutant alleles under the control of p*lin-31*.

Genotype	**Transgene**	**Multivulva (Muv) phenotype (%)**	**Vulvaless (Vul) phenotype (%)**	***N***
WT	-	0	0	>1,000
mpk-1(*pan14*[D321G])	-	0.5	0	1,000
WT	empty vector	0	0	231
WT	*MAPK1*^{WT}	0	0	639
WT	*MAPK1*^{I74N}	0.4	0	441
WT	*MAPK1*^{H80Y}	1.0[a]	0	479
WT	*MAPK1*^{A174V}	1.2[b]	0	651
WT	*MAPK1*^{D318G}	1.4[b]	0	370
WT	*MAPK1*^{P323R}	2.0[c]	0	492
let-23(sy1)	-	0	85.0	939
let-23(sy1); mpk-1(*pan14*[D321G])	-	0.9[d]	58.9[e] [*r*=30.7]	555
let-23(sy1)	*MAPK1*^{WT}	0	79.8[f] [*r*=6.1]	297
let-23(sy1)	*MAPK1*^{I74N}	0	78.0 [*r*=9.2]	295
let-23(sy1)	*MAPK1*^{H80Y}	0.7	70.7[g] [*r*=16.8]	300
let-23(sy1)	*MAPK1*^{A174V}	0.5	76.9 [*r*=9.5]	221
let-23(sy1)	*MAPK1*^{D318G}	1.1[d]	63.1[h] [*r*=25.8]	253
let-23(sy1)	*MAPK1*^{P323R}	0.7[d]	69.8[i] [*r*=17.9]	567

The c.962A>G variant leading to the p.Asp321Gly amino acid substitution, corresponding to the human p.Asp318Gly change, was introduced in the *C. elegans mpk-1* gene by CRISPR-Cas9. As a complementary approach, wild-type (WT) *MAPK1* and five disease-causing mutants were overexpressed under the control of the *lin-31* promoter, which drives expression principally in vulval precursor cells.

Multivulva (Muv) and vulvaless (Vul) phenotypes are expressed as percentage of adult animals displaying multiple ectopic pseudovulvae or lacking a vulva, respectively.

let-23(sy1) is a hypomorphic allele of *let-23*, homolog of the human gene encoding the EGF receptor. *N* indicates the number of animals scored; *r* specifies the rescue of the Vul phenotype associated with homozygosity for the *let-23*(*sy1*) allele expressed as percentage (|[%Vul/85-1]|x100). A single letter code is used to specify amino acid changes.

In all comparisons, *p* values were calculated using two-tailed Fisher's exact test.
[a-c] Significantly different from animals expressing *MAPK1*^{WT} ([a] $p < 0.02$; [b] $p < 0.01$; [c] $p < 0.0005$).
[d-f] Significantly different from *let-23(sy1)* animals ([d] $p < 0.02$; [e] $p < 0.00001$; [f] $p < 0.05$).
[g-i] Significantly different from *let-23(sy1*) animals expressing *MAPK1*^{WT} ([g] $p < 0.02$; [h] $p < 0.00002$; [i] $p < 0.002$).